Research article

Tectonic setting, provenance, depositional, and paleo-climatic conditions of the late quaternary subcrop sediments of the southeastern coastal region of the Bengal basin

Md. Bazlar Rashid [*], Md. Ahosan Habib, Arif Mahmud, Md. Kamrul Ahsan, Md. Hossain Khasru, Md. Ashraf Hossain, Aktarul Ahsan, Kazi Munsura Akther, Shawon Talukder

Geological Survey of Bangladesh, Dhaka, Bangladesh

ABSTRACT

This is a systematic attempt to depict the genetic evolution of the Late Quaternary sediments of the southeastern (SE) coastal region of the Bengal basin regarding paleotectonic settings, sedimentation, provenance, paleo-climatic conditions, weathering condition and age. The study has considered multiple attributes such as, lithology/lithofacies, sedimentary features/records, major oxides, clay minerals, foraminifera, and radiocarbon dating. The lithological characters along with associated clay minerals confirmed that a Pleistocene paleosol horizon (over-bank deposits) of warm-humid nature is commonly encountered immediately on top of the sub-crop bed-rock in the area overlain by Holocene fluvio-marine sediments of the same nature. The lithofacies, foraminiferal assemblages, and sedimentary structures of the analyzed samples suggest that the Holocene sediments have been presumably deposited in a fluvio-marine condition after the Last Glacial Maximum (LGM) due to the transgression of the sea. Geochemically, the sediments are classified as Fe-rich shale, shale, and wake and primarily intermediate to felsic orogen provenance. These are possibly derived from intense weathered sources from the upheaval of Himalayan ranges of both active continental margin and Island Arc paleotectonic setting. The plot of the Index of Compositional Variability versus the Chemical Index of Alteration indicates that the sediments seemingly experienced intense weathering associated with warm and humid climatic conditions. The sedimentation rates of the area vary from place to place and layer to layer due to the complex delta-building process. The reconstructed Relative Sea Level Curve reveals that presumably, the sea level has reached its current position after the LGM. The deduction possibly will facilitate the (1) reconstruction of Late Quaternary coastal evolution after LGM, (2) support for future urbanization, land use plans, etc., and (3) also be helpful for international researchers to understand the possible sources of sediment input in the area from the complex interplay of the Indian-, Eurasian- and Myanmar-plates.

---

* Corresponding author. Geological Survey of Bangladesh, 153-Pioneer Road, Segunbagicha, Dhaka 1000, Bangladesh.
E-mail address: bazlarrashid@ymail.com (Md.B. Rashid).

1. Introduction

Bangladesh covers the majority portion of the world's largest delta, namely the Ganges-Brahmaputra-Meghna Delta (also called Bengal Delta) (Fig. 1A [1–6]), which is more or less flat, sloping gently towards the south and finally merging with the Bay of Bengal. The country has a wide coast of approximately 710 km long coastline and an average elevation of 3 m above Mean Sea Level [7]. The coast has great significance regarding geology, geomorphology, geo-resources, livelihood, infrastructural development, tourism, and the rapidly growing economy of the country. However, it faces various challenges due to its geographic position, low elevation, frequent coastal inundation, random cyclone surge, land erosion, salinity, etc. [8-13]. Therefore, a sound understanding of the coastal processes, behavior, geo-environmental conditions and sedimentological and lithological characteristics for better coastal management and sustainable development of the coast integrated geological investigation is inevitable.

The geology, geomorphology, stratigraphy, landform evolution, tectonics, and depositional history of the Late Quaternary sediments of the delta were sparsely investigated by several researchers [4,14–20]. Coastal zone management and coastline changes with time in the delta were also performed by several authors [8,9]. Radiocarbon ages and the rate of accumulation of sediments in the delta were measured and calculated by different researchers [16,21,22]. Geology, geomorphology, geochemistry, changing geometry, coastal process, morphological evolution, and Holocene sea level changes of the Cox's Bazar area of the southeastern (SE) coastal part (Fig. 1A and B) of the delta were also sporadically conducted by several scholars: Hossain et al. [23] carried out compositional variations, chemical weathering, and provenance of sands from the beach of the SE coast of Bangladesh through major oxides, trace and rare earth element compositions analysis; Khan et al. [24] conducted the evolution of landforms and soils in a part of this coast during the Late Quaternary Period based on the degree of soil development and luminescence dating; Hasan and Hasan, Khan et al. and Ahsan et al. [25-27] carried out the geomorphology, changing geometry and morphological evolution of this coast based on morphology and lithology of the area; Ahsan and Rashid [28] carried out a coastal process on the basis of beach morphology, and erosion-accretion patterns of the coast; Monsur and Kamal [29] identified and described the signatures of Holocene Sea level changes along this coast with help of the Fairbridge (1962) world sea-level curve, etc. However, these studies lack any systematic interpretation of the paleotectonic settings, sedimentation, provenance, paleo-climatic conditions, weathering condition, radiocarbon ages and radiocarbon accumulation rate of the sediments of the SE coastal region of the Bengal Basin.

Therefore, the research gap inspires the authors to expedite the current research to systematically investigate its characteristic features considering multiple attributes (lithology, sedimentary features, major oxides, clay minerals, foraminifera, and radiocarbon dating) of the sediments. Clay mineralogy, geochemical properties, microfossil assemblages, and sedimentary structures can play an important role to unveil the depositional condition of the basin [30-42]. Hence, the research will supplement additional information about landform, tectonic setting, provenance, depositional, and paleo-climatic conditions of sediments of the SE coastal part of the Bengal basin. The study will also provide valuable insights to understand the sedimentation rate as well as Holocene sea level changes in the area similar to other deltaic parts of the Bengal basin. Moreover, the coastal region becomes the central hub for faster economic growth complimenting urbanization, industrialization, and intense agricultural activities of the country. Any development without the appropriate knowledge of those aspects could be socially-environmentally-economically deleterious. Therefore, the output of the
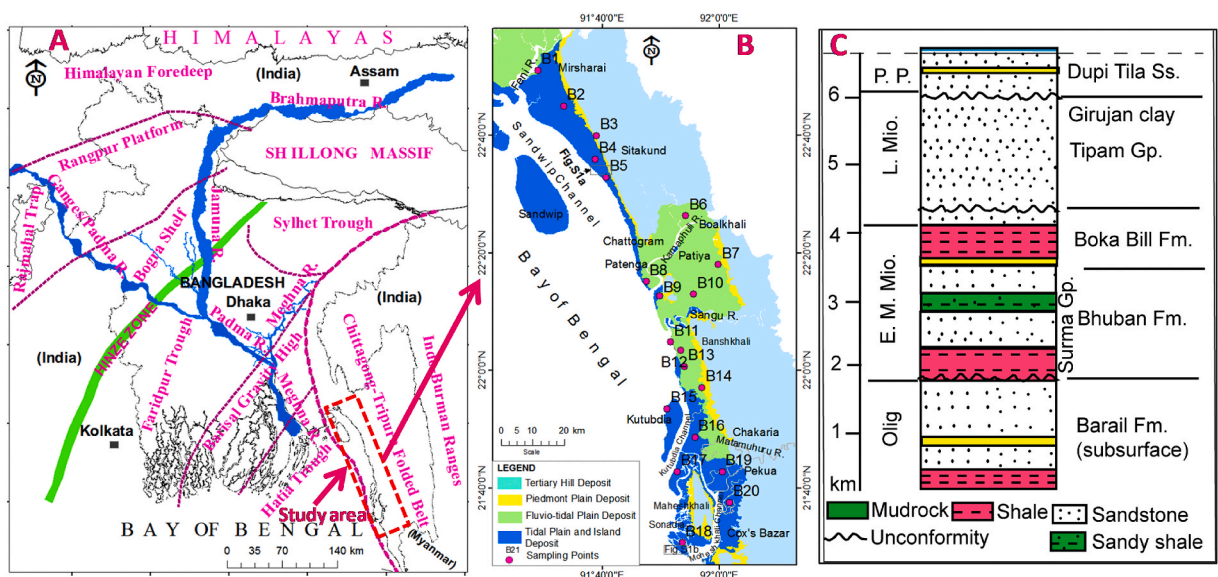
Fig. 1. (A) Regional map showing the location of the study area and major tectonic division of the Bengal Basin and surrounding areas (modified after [1,2]; Khandoker, 1989; [3]); (B), general geology with a distribution of borehole sites in the study area where the sediments samples were taken and profiles of lithological cross-sections; (C) the traditional stratigraphic units that are exposed in the Chittagong-Cox's Bazar Tertiary Folded Belt (CCTFB) [4-6].

research would be supportive of sustainable coastal management through vulnerability reduction, urbanization/-land use planning, disaster protection, balancing ecosystem, contamination prevention, etc. which affect the well-being. Therefore, the study objectives cover, but are not limited to: (1) describe lithological and sedimentological characteristics, (2) explain weathering and litho-stratigraphy of the area, (3) classification of sediments, (4) delineate sedimentation rates and sea level change, (5) determine provinces of sediments, depositional environment, and tectonic setting, and (6) understand the evolution process of the area. Finally, it will also be helpful for international researchers/readers to understand the possible sources of sediment input in the region from the complex interplay of the Indian-, Eurasian- and Myanmar plates [3,4,36,43], and also an evolution of the area.

2. Regional geologic setting

The area (coastal plain) lies along the eastern coast of Bangladesh which has the close vicinity of the SE Chittagong Tripura Folded Belt (CTFB) of the SE Bengal Basin (Bengal Foredeep) and immediately west of the Indo-Myanmar orogenic belt [3,44,45]. During the early Tertiary period, the Indian Plate drifted away from the Gondwana land in the Late Cretaceous, traveled towards the north, and collided with the Eurasian Plate and subsequently with the western part of the Myanmar Sub-plate, eventually forming the Bengal basin [43]. Structurally, the basin is bounded to the west by the Rajmahal Hills, to the east by the Fold Belt of the Indo-Myanmar Ranges, to the north by the Himalayan Foredeep, the Shillong Massif and the Assam Basin, and is open in the south as the Bengal Fan [2,3,44–49] (Fig. 1A). It is a complex and asymmetric collisional foreland basin, exhibiting intense changeability in Neogene sediment thickness, having thinner, gently sloping sediment cover in the western and northern parts, and thicker in a basin-ward way to the south and southeast reflecting a complex depositional environment and tectonics [4,34–36,50–52]. However, this is the thickest sedimentary basin in the world nearly 21 km thick [43] (Fig. 1C).

The configuration of the basin and its sedimentary fill are closely connected to the world's largest Himalayan-Tibetan orogenic system, covering approximately 20 million km^2 of area. The huge sediment thickness in the basin is the consequence of tectonic mobility or instability of the areas causing quick subsidence and sedimentation in a relatively short duration of geologic time [3,53]. The collective sediment dispersal through the basin into the Bay of Bengal per year is projected to be approximately 1.1 Gigaton and consequently formed the biggest submarine fan in the world, the Bengal Fan [43,54]. The basin traps and accumulates less than half of the total sediment budget through flexural subsidence over a large area, in addition to faulting, folding and localized compaction [55]. It is occupied mainly by the Bengal Delta. The delta plains are extended over parts of the Indian states of West Bengal in the west, a vast region of Bangladesh in the middle, and Tripura in the east [45]. The major progradation of the delta continued to the south into the Bay of Bengal and has developed a wide coast. Geographically, the SE coastal segment of the country lies in front of the CTFB of Bangladesh which is characterized by tidal and fluvio-tidal plains and coastal Islands with many beaches (Fig. 1B; Fig. S1A, B).

The CTFB is the only tectonic element of the country that was uplifted into a hilly landform incorporating itself into a frontal belt of the Indo- Myanmar Orogeny to the east. It is one of the active collisional orogenic belts in the world [3,44,45]. Structural (folding,
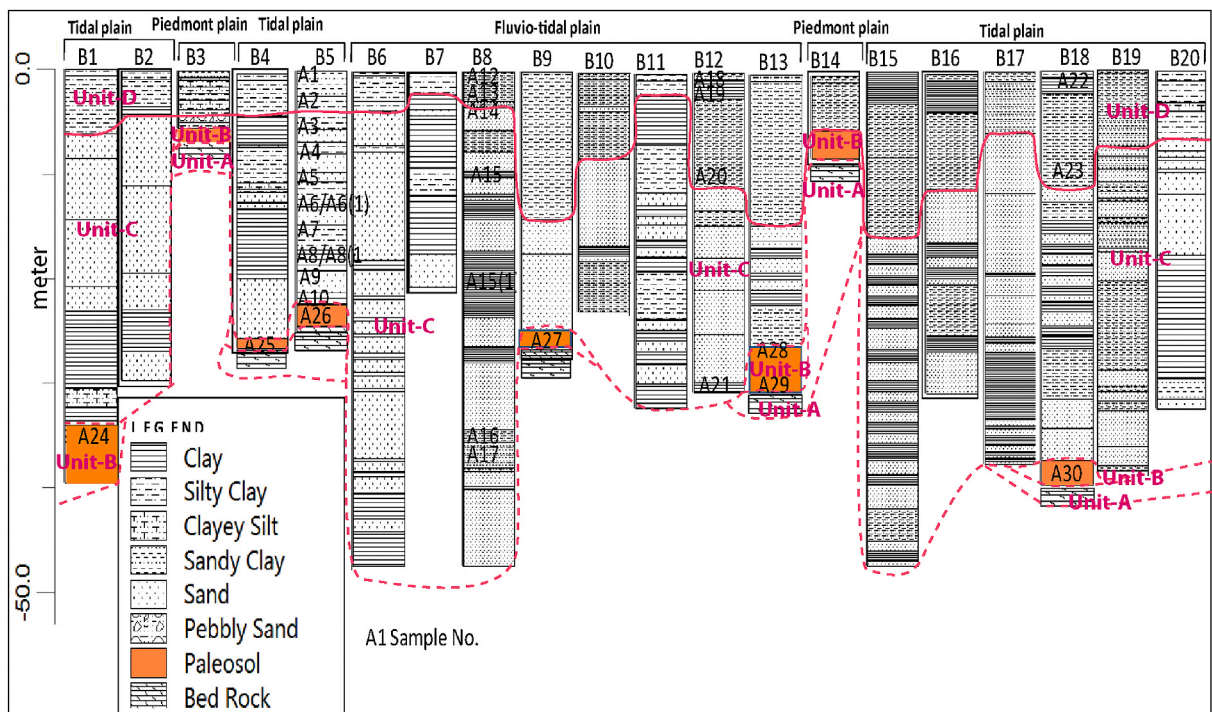

Fig. 2. Lithologs and lithostraigraphic units of studied boreholes.

faulting) growth in the belt may have started during the Pliocene and is still active [3,44,45]. The piedmont plains sporadically appear in the area (Fig. 1B, Fig. S1A). The sediments of the Feni, Karnaphuli, Sangu, and Matamuhuri rivers have been deposited along the coast and around the offshore islands resulting in their growth into the sea through fluvial and tidal processes.

3. Materials and methods

3.1. Sampling

The sedimentary characteristics, up to a depth of 50 m, of various geomorphic units were unveiled using traditionally employed borehole techniques according to Ref. [56]. For lithological inspection, 20 boreholes (Bore hole ID: B 1–B 20) (Figs. 1 and 2) were drilled. Representative sub-crop sediment samples (n = 33; 26 samples from Holocene sediments and 7 samples from Pleistocene weathered (paleosol) sediments) were systematically and carefully collected, intensively studied, and recorded in detail onsite. The study particularly investigated some typical attributes e.g. lithology, lithofacies-distribution-classification-association, sand/clay ratio, color, texture, sorting, angularity, structure, stickiness, compactness of samples from varied depths by Chopping method (shallow tubewell sinking) (depth: 10–50 m, continuous sampling), Standard Penetration Technique (SPT) (30 m; sampling interval 1.5 m) techniques and excavation of pits (1.0–1.5 m). The samples were immediately preserved in tightly packed bags and transferred to the laboratory for further analysis.

3.2. Geological map preparation and lithofacies analysis

A geological map (Fig. 1B) of the area was prepared based on a Landsat L8 image captured on 10 May 2020 encompassing the field observations, and other relevant data (e.g., lithologic, sedimentologic, and geomorphic data, etc.), as well as available published information. The image enhancement, layer stack and mosaic of images were done with Erdas Imagine 2010 and Arcmap 10. The visual image interpretation [57] was used to delineate the various geological units, as it is viewed as a standard practice in previous works [8,58–60]. Positions of sampling sites were recorded with GPS and then incorporated into the produced map. The lithostratigraphy (Figs. 2 and 3) of the region was evaluated based on lithological, sedimentological, mineralogical, age similarity, and ultimately the study proposed litho-stratigraphy of the area.

Fig. 3. Generalized litho-stratigraphy of the SE Coast of Bangladesh; (A) exposed tidal rhythmites at Kutubdia Island; (B) Mud-draped cross strata at Cox's Bazar, coast; (C) tidal rhythmites structure and (D) alteration of sand and clay collected from the subsurface sediments samples of the SE Coast; (E) weathered sediments at about 25.30 m depth (Sample No. A26).

3.3. Major oxides analysis

Concentrations of eight major oxides of the elements Si, Al, Fe, Ti, Ca, Mg, K, and Na of the representative composite samples from different samples (n = 33; 26 samples from Holocene sediments and 7 samples from Pleistocene weathered (paleosol) sediments) of different boreholes (Figs. 1B and 2; Tables S5 and S6) were carefully and accurately measured at the Analytical Chemistry Laboratory of the Geological Survey of Bangladesh (GSB) following the standard procedures of Ref. [61].

3.4. Clay mineral analysis

The X-ray diffraction (XRD) technique (Phillips X-Pert Pro, Panalytical, Netherland) was applied to analyze sixteen selected silty clay samples (n = 16; 14 samples from Holocene sediments and 2 samples from Pleistocene weathered (paleosol) sediments) (Table 1; Figs. 1 and 2) at GSB for identifying the clay minerals. The procedures and peak behaviors as stated by Refs. [62–68] were followed to identify different groups and types of clay minerals. The semi-quantitative method was applied to quantify the proportion of individual minerals present in a sample. The area under each peak was calculated by multiplying the peak height from by a common base line with the half-height width. The calculated peak areas were then multiplied by their corresponding weighted factor to make a direct comparison of their peak areas more reasonably [69]. Finally, the relative percentage was calculated for each clay mineral group present in a sample by comparing the weighted peak areas.

3.5. Biofacies analysis

Twenty mud-rich (silty clay, clay) samples (n = 20; Holocene sediments) (mud-rich) from different depths (m) of different boreholes (Table 2; Figs. 1 and 2; Tables S1–S4) were considered for analysis. A total of 100 g samples were obtained from each representative sample. Then it was treated with hydrogen peroxide and Glauber salt. Afterward, it was washed through a 0.063μm sieve under low water pressure. The sand fractions were then collected and dried at 60 °C in an oven. Finally, the Foram specimens Species (Fig. 4, [70–72]) in the dried samples were identified and quantified under an Olympus SZ stereo binocular microscope. Around 300 foraminifera were picked up and identified following the generic classification of Ref. [71,73–76]; and http://www.foraminifera.org/.

3.6. ^{14}C dating, sedimentation rates estimation, and relative sea level curve (RSLC) construction

Radiocarbon ages of four selected shell and wood fragment samples (n = 4) with respective litholog ID (Table 3; Figs. 1 and 2) were dated with Accelerator Mass Spectrometry at the RAFTER GNS SCIENCE, New Zealand. Then the measured ages were converted to calendric ages by CalPal online software calibration. Calibration is needed, because a key element in calculating radiocarbon ages is the atmospheric $^{14}C/^{12}C$ ratio, which is not constant historically [77]. Then the sedimentation rates were calculated from the depth of measured dated material divided by calibrated calendric age. In the case of marine shells, the average marine reservoir effect (158 ± 68 years) of the Indian Ocean [78] was subtracted from the radiocarbon age, and then calculated as the calendric age (calBP). Radiocarbon ages of different sediment samples of the other areas (deltaic coast) of the delta were also collected from published literature and converted to calendric ages. Afterward, the sedimentation rates were calculated. RSLC was reconstructed considering the obtained ages and available literature age data as shown in Fig. 5. It is worth mentioning that the exact elevations of the sampling sites were not available. Hence, an average value of about 2 m (generalized elevation of the coast of Bangladesh) was considered to estimate the sample depth. In this regard, there is a possibility of a minor deviation of exact sample depths from the present sea level.

Table 1
Relative Abundance of Clay Minerals in sediments of different boreholes in the study area (Figs. 1 and 2).

Borehole	Sample no.	Depth (m)	Litho type	Relative abundance (%)			
				Vermiculite	Chlorite	Illite	Kaolinite
B5	A2	4.25	Silty clay	–	24.50	57.50	18.00
	A7	15.00	Clayey silt	–	24.50	57.10	18.40
	A8	17.50	Clayey silt	–	11.25	61.50	27.25
	A10	22.55	Sandy silt	–	16.30	58.60	25.10
	A26	25.30	Sandy silt	22.2	–	57.30	20.50
B8	A12	0.50	Silty clay	–	21.50	57.30	11.20
	A13	1.5	Silty clay	–	23.20	58.50	18.30
	A14	6	Silty clay	–	24.40	57.30	18.30
	A16	35	Silty clay	–	15.25	61.55	23.20
B12	A18	.50	Silty clay	–	23.60	57.40	19.00
	A19	2.5	Silty clay	–	22.50	59.30	18.20
	A20	13.0	Silty clay	–	21.25	57.50	21.25
	A21	32	Silty clay	–	24.10	57.30	18.60
B18	A22	1.52	Silty clay	–	24.20	56.40	19.40
	A23	9.14	Silty clay	–	16.25	60.50	23.25
	A30	39.62	Silty clay	20.2	–	58.30	21.50

Table 2
Presence of Foraminifera in the unconsolidated sediments of the SE coast.

| Borehole	Sample no.	Depth (m)	Presence of Microfossils
B5	A1	0.50	*Ammonia baccarii, Ammonia dentate, Nonionella* sp., *Quinqueloculina* sp., *Spinorotalia himchari*
	A2	4.25	*Ammonia baccarii, Ammonia dentate, Elphidium macellum, Spiroculina* sp., *Biloculina* sp., *Cyclammina* sp., *Amphistigina* sp., *Woodela* sp., *Spinorotalia himchari*
	A3	5.5	*Ammonia baccarii, Ammonia dentate, Elphidium macellum, Nonionella* sp., *Quinqueloculina* sp., *Globigerina bulloides, Triloculina* sp., *Spinorotalia himchari*
	A4	7.00	*Ammonia baccarii, Ammonia dentate, Elphidium macellum, Nonionella* sp., *Bolivina* sp., *Quinqueloculina* sp., *Globigerina bulloides, Spiroculina* sp., *Alveolinella quoyi, Cyclammina* sp., *Amphistigina* sp., *Woodela* sp., *Spinorotalia himchari*
	A5	10.00	*Ammonia baccarii, Ammonia dentate, Elphidium macellum, Quinqueloculina* sp., *Triloculina* sp., *Spiroculina* sp., *Cyclammina* sp., *Amphistigina* sp., *Woodela* sp., *Spinorotalia himchari*
	A6	12.00	*Ammonia baccarii, Ammonia dentate, Elphidium macellum, Nonionella* sp., *Quinqueloculina* sp., *Triloculina* sp., *Biloculina* sp., *Spiroculina* sp., *Cyclammina* sp., *Spinorotalia himchari*
	A7	15.00	*Ammonia baccarii, Ammonia dentate, Quinqueloculina* sp., *Triloculina* sp., *Spiroculina* sp., *Cyclammina* sp., *Woodela* sp., *Spinorotalia himchari*
	A8	17.50	*Ammonia baccarii, Ammonia dentate, Quinqueloculina* sp., *Triloculina* sp., *Cyclammina* sp.
	A9	20.70	*Ammonia baccarii, Ammonia dentate, Elphidium macellum, Nonionella* sp., *Quinqueloculina* sp.,
	A10	22.55	*Ammonia baccarii, Ammonia dentate, Elphidium macellum, Quinqueloculina* sp.
B8	A12	0.50	*Ammonia baccarii, Ammonia dentate, Nonionella* sp., *Quinqueloculina* sp.
	A13	1.5	*Ammonia baccarii, Ammonia dentate, Elphidium macellum, Spiroculina* sp., *Cyclammina* sp., *Amphistigina* sp., *Woodela* sp.; *Spinorotalia himchari*
	A14	6	*Ammonia baccarii, Ammonia dentate, Elphidium macellum, Nonionella* sp., *Quinqueloculina* sp., *Globigerina bulloides, Spinorotalia himchari*
	A16	35	*Ammonia baccarii, Ammonia dentate, Elphidium macellum, , Quinqueloculina* sp.
B12	A18	0.5	*Ammonia baccarii, Ammonia dentate, Nonionella* sp., *Spinorotalia himchari*
	A19	2.5	*Ammonia baccarii, Ammonia dentate, Elphidium macellum, Biloculina* sp., *Cyclammina* sp., *Amphistigina* sp., *Woodela* sp., *Spinorotalia himchari*
	A20	13	*Ammonia baccarii, Ammonia dentate, Elphidium macellum, Nonionella* sp., *Triloculina* sp., *Biloculina* sp., *Spiroculina* sp., *Cyclammina* sp., *Spinorotalia himchari*
	A21	32	*Ammonia baccarii, Ammonia dentate, Quinqueloculina* sp.
B18	A22	1.52	*Ammonia baccarii, Ammonia dentate, Nonionella* sp., *Spinorotalia himchari*
	A23	9.14	*Ammonia baccarii, Ammonia dentate, Elphidium macellum, Spiroculina* sp., *Amphistigina* sp., *Woodela* sp., *Spinorotalia himchari*

4. Results

4.1. Litho-stratigraphy

Based on borehole data and lithologic characteristics, stratigraphically the SE coastal zone is divided into four lithostratigraphic units (A to D) (Figs. 2 and 3). Unit-A is the lowermost unit in the study area. This unit is composed of gray, bluish-gray colored shale and brownish-gray colored sandstone of Miocene age. Shale is laminated, and fissile whereas sandstone is bedded, very hard, and compact. This unit is overlain by Unit-B which is composed of greenish gray, olive gray, very dark grayish brown, dark brown, yellowish brown, light yellowish brown colored moderately compact to very hard and compact clayey silt/silty clay (weathered horizon/paleosol) of the Pleistocene age. It is sticky in nature, feels soapy and presents concretions. The thickness of the unit varies from 1 to 3 m. Unit-B is overlain by Unit-C which is composed of thick sand or alteration of sand and clay of the Holocene age. Sands of Unit-C are light olive gray to gray colored, fine to medium-grained, moderately sorted, and sub-angular to sub-rounded, while clays are dark gray, soft, and sticky. Roots, rootlets, and traces of decomposed vegetal matter are present. The thickness of this unit varies from 10 to 45 m. The upper most lithostratigraphic unit in the study area, Unit-D, is composed of light olive gray, light olive brown, and light yellowish brown-with light gray, gray, grayish brown, dark reddish brown, dark grayish brown, yellowish brown, and dark gray colored clayey silt and silty clay of the Holocene age. These sediments are slightly compacted and friable under hand pressure. The deposits contain decomposed and partially decomposed vegetal matter, iron concretions, iron spots, roots, rootlets, and oxidation along roots and rootlets. In some places, these deposits contain dark brown to black colored peats. The peats are fibrous, decomposed, sometimes partially decomposed, and occasionally contain wood fragments. The thickness of this unit varies from 5 to 15 m.

4.2. Chemical composition of sediments

The Holocene sediments have low concentrations of SiO_2 ranging from 50 to 73.3 wt% (average 60 wt%, σ = 5, Table S5). The average value of silica (60 wt%) is far less than upper continental crust (UCC) followed by higher Al_2O_3 and Fe_2O_3 contents (11.9–21.5 and 4 to 12.6; average 17.3, 7 wt%, and σ = 2.90, 1.63, respectively) compared to UCC values. The sediments have also low concentrations of TiO_2, MgO, CaO, Na_2O, and K_2O ranging from 0.3 to 0.8, 1 to 3.6, 0.2 to 1.3, 0.6 to 1.2 and 1.6 to 2.8 wt% (average 0.6, 2.34, 0.5, 1.0, 2.4 wt%, and σ = 0.13, 0.61, 0.37, 0.19, 0.35, respectively) compared to UCC values. The Pleistocene sediments have also low concentrations of SiO_2 ranging from 54.3 to 62.1 wt% (average 59 wt%, σ = 3.1, Table S6). The average value of silica (59 wt %) is also much less than UCC followed by higher Al_2O_3 and Fe_2O_3 contents (15.5–21.5 and 5.2 to 8.2; average 18.1, 7.1 wt%, and σ = 2.3, 1.6, respectively) which are nearly similar to UCC Holocene sediments. However, the concentrations of Al_2O_3 and Fe_2O_3 are much
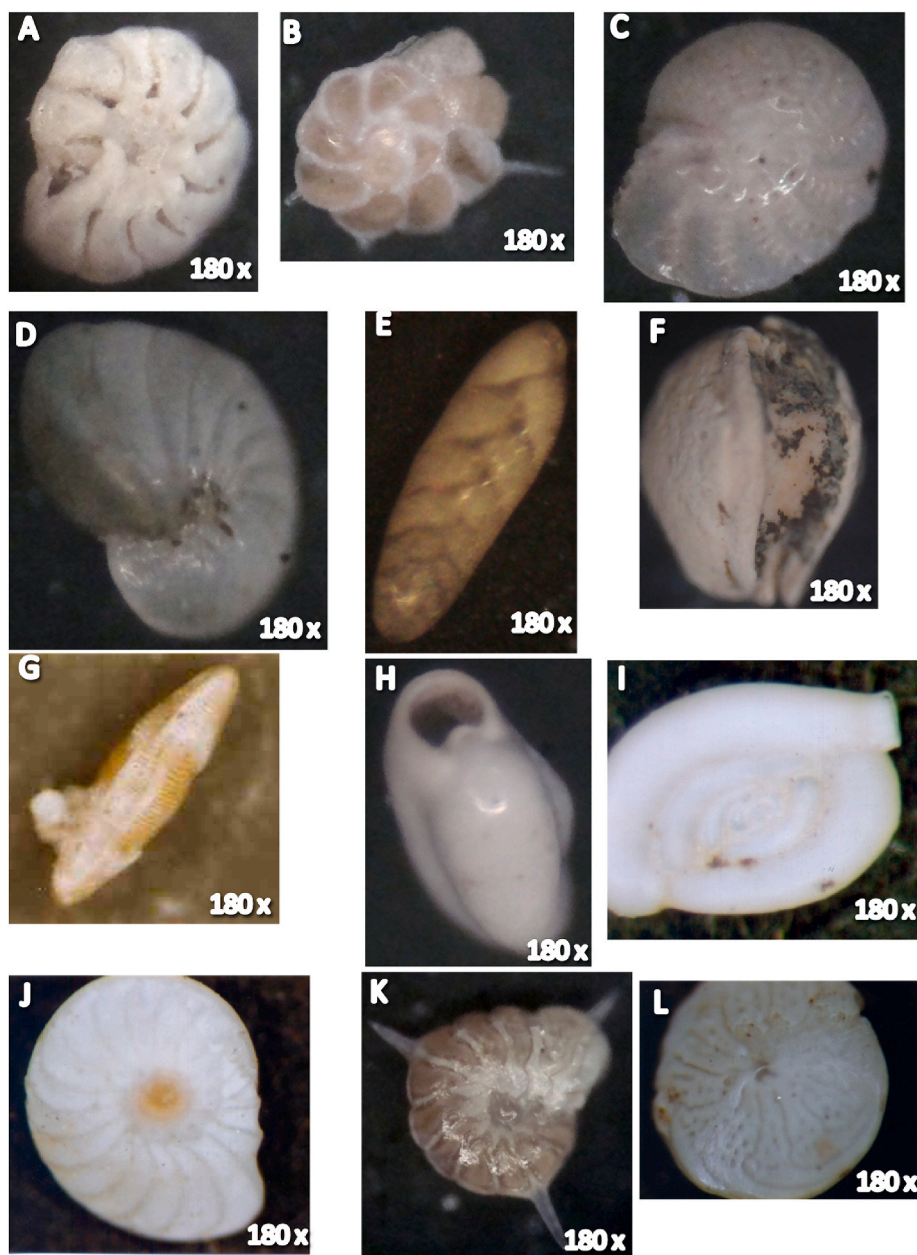
Fig. 4. (A) Ammonia beccarii (Linne, 1758); (A) Ammonia dentate (Linne, 1758); (C) Elphidium macellum; (D) Nonionella sp. (Cushman, 1927); (E) Rotaliina [70]; (F) Quinqueloculina sp.; (G) Alveolinella quoyi (Douville, 1906 (Source: [71]); (H) Triloculina sp.; (I) Spiroculina sp.; (J) Cyclammina sp; (K) Spinorotalia himchari [72]; (L) Amphistigina vulgaris.

higher than in the recent sediments. The sediments have also low concentrations of TiO_2, MgO, CaO, Na_2O and K_2O ranging from 0.6 to 0.8, 0.8 to 2.8, 0.2 to 1.7, 0.6 to 1.2 and 1.8 to 2.6 wt% (average 0.7, 1.8, 0.7, 0.9, 2.3 wt%, and σ = 0.1, 0.7, 0.6, 0.3, 0.3, respectively) compared to UCC values.

4.3. Clay mineralogy

The Chlorite, illite, and kaolinite group have been identified in the analyzed samples (Table 2). Two distinct suites of clay minerals are present: (1) Suite-I: consists of vermiculite-illite-kaolinite in the case of the samples collected from the Pleistocene weathered (paleosol) sediments, and (2) Suite-II: comprised of chlorite-illite-kaolinite from the samples collected from the Holocene sediments. The results also show that all the samples are free from mica. However, the samples contain a significant amount (57.1–61.5%) of illites.

Table 3

Radiocarbon ages of the deltaic and the results of radiocarbon dating of the southeast coast of Bangladesh compared with literature age data available from Bengal Delta.

Area	Borehole/Sample No.	Depth (altitude) (m)	Material	Measured radiocarbon age (yrs BP)	Calendric Age cal BP	Accumulation rate (mm.yr^{-1})
Sitakund, Chittagong Bangladesh[a]	B5/A9	20.70	Shell	5232 ± 25	5832 ± 33	3.44
Patenga, Chittagong Bangladesh[a]	B8/A15	13.41	Wood	1164 ± 20	1095 ± 38	12.25
Patenga, Chittagong Bangladesh[a]	B8/A17	37.80	Wood	$10,999 \pm 40$	$12,912 \pm 99$	*2.06
Banskhali, Chittagong Bangladesh[a]	B12/A21	32.00	Wood	8326 ± 25	9364 ± 44	3.42
Sankrail, Howrah, Calcutta, India[b]	TF-850	1.37	Peat	2615 ± 100	2676 ± 147	0.51
	?	1.52	Wood	4925 ± 100	5708 ± 117	0.27
	TF-851	1.82	Peat	4075 ± 100	4613 ± 153	0.39
	TF-855	3.04	peat	4720 ± 135	5414 ± 163	0.56
	?	4.87	Wood	5440 ± 115	6205 ± 139	0.78
	TF-856	6.25	Peat	5810 ± 120	6622 ± 125	0.94
Sirajganj, Rangpur, Bangladesh[c]	GaK-5158	112 (−101)	Wood	$28,320 \pm \frac{1750}{1440}$	$32,801 \pm 1504$	3.41
					$32,847 \pm 1181$	
Kanaighat, Sylhet, Bangladesh[c]	GaK-11955	8.55	Peat	4180 ± 120	4696 ± 147	1.82
Dewlatpur, Khulna, Bangladesh[d]	GaK-12952	5 (−3)	Peat	3230 ± 110	3474 ± 120	1.44
	NUTA-342	16 (−14)	Wood	$6,490 \pm 100$	7401 ± 88	2.16
	GaK-12953	13 (−11)	Wood	6880 ± 130	7742 ± 118	1.68
	NUTA-343	27 (−25)	Wood	7640 ± 100	8456 ± 85	3.19
	NUTA-344	34 (−32)	Plant	$8,890 \pm 150$	9950 ± 212	3.42
	GaK-12954	30 (−28)	Wood	$10,190 \pm 210$	$11,908 \pm 429$	2.52
	NUTA-345	48 (−46)	Plant	$12,320 \pm 240$	$14,535 \pm 481$	3.30
Bangladesh[e]	NUTA-1342	20 (−18)	Shell	7060 ± 120	7878 ± 114	2.54
	NUTA-1345	35 (−32)	Shell	$8,910 \pm 150$	9968 ± 211	3.51
21°49′25″–90°08′12″[f]	6BP98	1.5	Buried Tree	495 ± 45	614 ± 14	2.44
22°07′46″–89°42′56″[f]	19BS98	1.4	Marine Shell	1200 ± 30	730 ± 59	1.92
21°49′06″–89°27′37″[f]	7BS99	0.7	Wood	90 ± 40	227 ± 48	3.08

Area	Borehole/Sample No.	Depth (altitude) (m)	Material	Measured radiocarbon age (yrs BP)	Calendric Age cal BP	Accumulation rate (mm. yr^{-1})
21°49′06″–89°27′37″[f]	7BS99	2.2	Crab Claw	127 ± 7	309 ± 8	7.12
22°04′55″–89°13′30″[f]	12BS99	1.5	Peat	570 ± 50	584 ± 64	2.57
22°04′55″–89°13′30″[f]	12BS99	3.2	Peat	2300 ± 40	2378 ± 29	1.35
22°04′55″–89°13′30″[f]	12BS99	5.8	FW Shell	2690 ± 40	3192 ± 17	1.82
21°37′–88°18′[g]	BS1159	8.4	Wood	4710 ± 120	5430 ± 230	1.55
22°14′–88°47′[h]	SH9	4.9	Wood	4250 ± 40	4889 ± 61	1.00
21°45′–88°15′[i]	Gm7137	1.8	Kankar	3170 ± 70	3382 ± 144	0.53
22°33′–88°03′[j]	BVC16	1.1	Peat	910 ± 60	820 ± 111	1.34
22°32′56″–90°05′56″[k]	VC16	3.2	Peat	2120 ± 70	2267 ± 47	1.41
21°37′–88°18′[l]	OS19420	12.2	Wood	4790 ± 30	5582 ± 63	2.19
21°37′-88°18′[l]	OS16697	23.4	Shell	6040 ± 35	6921 ± 85	3.38
22°14′–88°47′[m]	BS1156	22.3	Wood	$7,530 \pm 180$	8748 ± 13	2.55
22°10′–88°38′[m]	BS1160	31.7	Wood	$6,250 \pm 140$	7137 ± 288	4.44

Notes: Depth (col.3) divided by calibrated calendar age (col.6) = annual change in land levels relative to mean sea-level; *24.39 m of sediments have been deposited between the depths of 13.41 m and 37.80 m; average rate of deposition of the area was 5.29 mm.yr^{-1} and in the deltaic part the average rate of deposition was 2.16 mm.y^{-1}.

[a] The study.
[b] [79].
[c] [14].
[d] [15].
[e] [16].
[f] [21].
[g] [80].
[h] [81].
[i] [82].
[j] [83].
[k] [18].
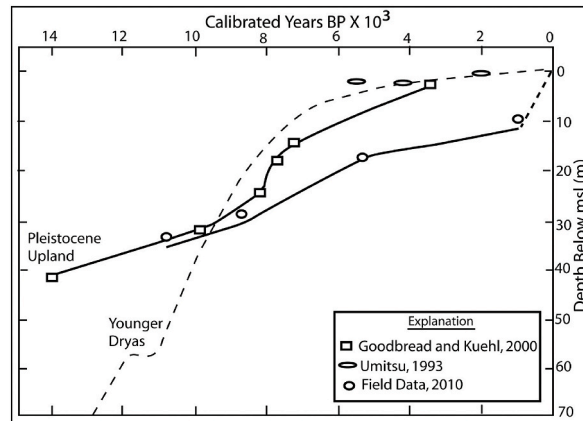
^l [81].
^m [80].

Fig. 5. Schematic illustration showing Reconstructed Sea Level Curve for the SE coastal part of Bangladesh.

4.4. Foraminifera

A total of 13 species of Foraminifera belonging to 9 genera under 3 suborders have been identified within the Holocene sediments of depths ranging from 1 to 22.6 m (Table 2; Fig. 4). Sample-wise abundances of forams are shown in Table 2.
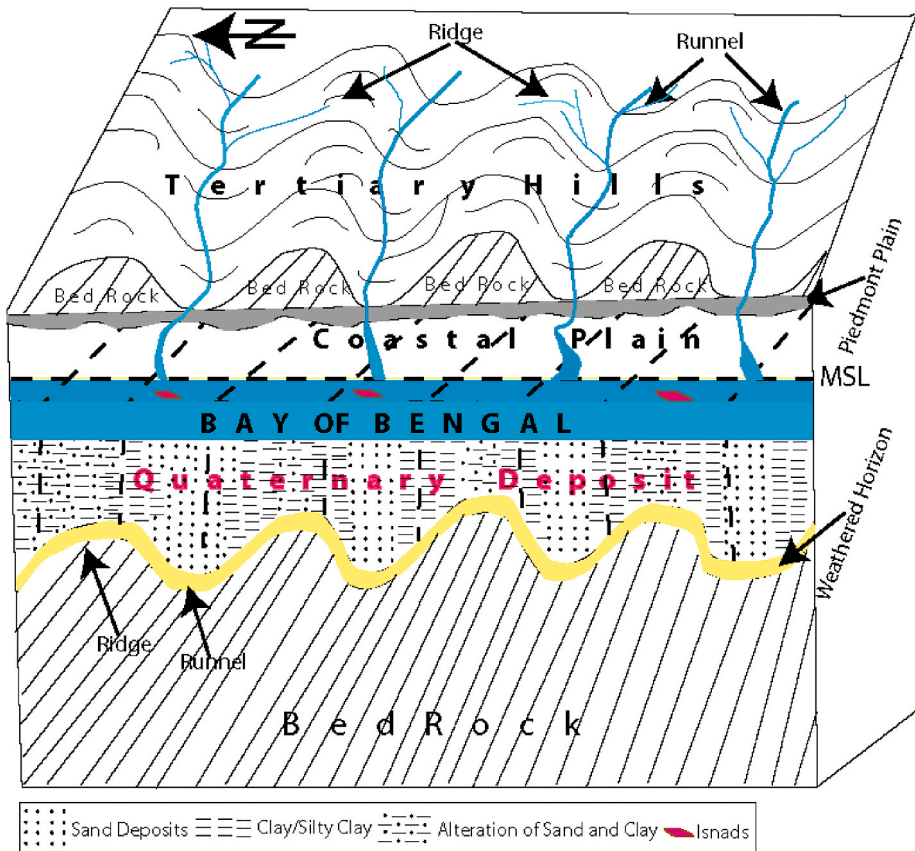

Fig. 6. Schematic illustration of the study area.

4.5. Radiocarbon ages and rate of deposition

One shell sample from Nonabil of Sitakund (Borehole B5; Figs. 1B and 2) with a depth of 20.7 m (Table S1; Table 3; Sample No. A9) was dated. The Radiocarbon age is 5232 ± 25 yrs BP and the calendric age is 5832 ± 33 calBP. It can be deduced that a thick layer of sediments (about 20.7 m) was deposited within 5832 yrs, and the estimated rate of deposition was approximately 3.4 mm yr^{-1} (Table 3). Two wood samples (Borehole B8; Figs. 1B and 2; Table S2; Table 3; Sample No. A15, A17) from Patenga, Chittagong (Chattogram) with depths of 13.4 m and 37.8 m were also analyzed. The measured and the calendric age of the two samples are 1164 ± 20 yrs BP and 1095 ± 38 calBP, and 10,999 ± 20 yrs BP and 12,912 ± 99 calBP, respectively. These measured ages indicate that approximately 24.4 m (37.8–13.4 m) thick sediment was deposited in 11,817 yrs (12,912–1095). And probably the corresponding rate of deposition was about 2.1 mm yr^{-1}. But in the upper part of the unconsolidated sediment of the area, the rate of deposition was tremendously high in comparison with the lower part. Approximately 13.4 m thick sediments were deposited in 1095 yrs suggesting the probable rate of deposition of about 12.3 mm yr^{-1} (Table 3). Another wood sample (Borehole B12; Figs. 1B and 2; Table S3; Table 3; Sample no. A21) from the Banskhali area with a depth of 32 m was also dated. The determined age of the sample is 8326 ± 25 yrs BP and the calendaric age is 9364 ± 44 calBP. Approximately 32 m thick sediment was deposited in 9364 yrs indicating the estimated rate of deposition around 3.4 mm yr^{-1} (Table 3). The average rate of sedimentation of the SE coast was 5.3 mm yr^{-1}. The results of radiocarbon dating of the SE coast of the country and radiocarbon ages available on the other part of the delta were compared (Table 3). In the other part, the average rate of sedimentation was 2.16 mm yr^{-1}.

4.6. Sea level curve

The reconstructed RSLC (Fig. 5) resembles the proposed curve by Refs. [15,16]. Though, the upper half of the curve corresponds well to the curve reconstructed by Ref. [18].

5. Discussion

*5.1. Depositional environment, lithofacies, source of sediments, and tectonic settings*

The CTFB is characterized by a series of long curvilinear anticlines and synclines [45] (Fig. 6). But the intensity of folding gradually increases eastwards, causing a higher topographic elevation on the eastern side of the folding belt. On the other hand, folding intensity decreases westwards and consequently merges into the recent coastal plain. The extension of the Tertiary bed-rocks was observed at the bottom of the unconsolidated coastal deposit along the southeast coast of the country (Figs. 2 and 6). The sediment characteristics suggest that a paleosol layer (weathered sediments) of about 1–3 m thick (Fig. 2) of Pleistocene age was encountered at a depth of 10–25 m over the Tertiary bed-rock. During the LGM (18,000 BP) when the mean sea level was approximately 100–130 m below its present condition and the coast was far away (about 250 km) from its present location [29], the area was exposed for a long period. Thus an extensive oxidized and weathered thick soil horizon locally regarded as paleosol was developed within bed-rock and Holocene unconsolidated sediments. After that when the sea level started rising, the recent sediments (Holocene sediments) (Figs. 2 and 3) (thick sands and alteration of sand and clay) along the coast started to deposit on that paleosol floor along with the influences from paleo- and present active GBM river systems under tidal condition. During or following these phenomena, several isolated offshore islands began forming over the erosional Tertiary bed-rock under sub-tidal conditions (e.g., Kutubdia, Sonadia, Sandwip, etc.). The Chemical Alteration (CIA) [84] values of the Pleistocene sediments range from 80.6 to 84.6 (σ = 1.5) (Table S6) which also indicate the hot and humid climatic conditions and extreme weathering. The CIA values of the Holocene sediments range from 77.8 to 84.3 (σ = 1.86) (Table S5) which indicates the warm humid climate conditions and intermediate weathering.

The clay minerals in deltaic sequences are detrital in origin, and they strongly reflect the character of their genetic history and are only slightly modified in their depositional environments [85,86]. In the present research, the identified Illite is the most abundant component in the analyzed samples (range: 57.1–61.5%, mean: 58.4%, σ = 1.59) (Table 1). It is worth noting that the illites are dominant clays in argillaceous (mud or clay-rich) rocks, formed by the intense weathering of silicates (primarily feldspar) group minerals, by the alteration of other clays, and during the degradation of muscovite [32,37]. ICV (Index of Compositional Variability) [87] values of the Pleistocene sediments range from 0.6 to 0.8 (σ = 0.1) (Table S6), and for the Holocene sediments range from 0.6 to 1.0 (σ = 0.13) (Table S5), which also indicate the feldspars group of minerals [87]. The formation of illites is generally favored by alkaline conditions and by high concentrations of Al and K [32]. Therefore, it can be depicted from here that synsedimentary feldspar and muscovite (mica) detrital minerals deposited (syngenetic process) initially with the sediments might have altered or degraded to illites (epigenetic and diagenetic processes) from muscovite [88] under saline water i.e., a tidal condition which enriched the abundances of the mineral group in sediments. Illite is any of a group of mica-type clay minerals widely distributed in marine shales and related sediments [32].

The well-developed distinct typical structures, like mud-draped cross strata (Fig. 3B), tidal rhythmites (alteration of thinly laminated silty clay and fine-grained sand) (Fig. 3A, C) within the sequence indicate the dominance of tidal influence in transitional (shallow marine to coastal) settings. Mud-draped cross strata are formed due to alternate bed form migration during the strong current/high flow velocities of different rivers and mud deposition during high or low tide [89]. Conversely, tidal rhythmites are packages of laterally and/or vertically accreted, laminated to thinly bedded fine-grained sand, silt, and clay of tidal deposits [90,91]. It forms especially in the intertidal zone, supratidal zone, and salt marshes or mangroves where clay or silty clay or peats accumulate. It represents continuous deposition over several years at a rate of a few decimeters per year [90].

The identified foraminifera are mainly benthic types that indicate a shallow marine environment except for *Globigerina bulloides*. Relative to the benthic species, the percentage of planktonic species, which indicates a deep marine environment, is very low. In the study area, the abundant foraminiferal species are *Ammonia beccarii, Ammonia dentate,* and *Asterorotalia trispinosa.* Other common species are *Elphidium macellum, Quinqueloculina* sp., *Cyclammina* sp. *Woodela* sp., *Alveolinella quoyi* (Table 2). The remaining species are rare in their abundance. All the identified fossils suggest that these are the fossils of a salinity range of 0–35‰ and a temperature range of 5–35 °C [92].

Geochemical results disclosed that the average values of silica (60 wt% ($\sigma = 5$) in recent sediments and 59 wt% ($\sigma = 3.1$) in Pleistocene sediments) are far lower than UCC, -signifying the destruction of feldspar during transportation, sorting, and recycling (Tables S5 and S6). Possibly, the illitization process turns the sediments free from mica [32,37]. The sedimentological study also exposed the three main lithofacies containing Fe-rich shale, shale, and wake (Fig. 7A, [93–95]). Like illite, the kaolinite group is also present in all analyzed samples. It is known that http://pubs.usgs.gov/of/2001/of01-041/htmldocs/images/kaoxtl.jpg all the members of the kaolinite group are formed primarily during hydrothermal alteration or weathering of feldspars under acidic conditions [32, 68]. In this regard, it can be considered that the kaolinite might have originated under a continental environment and remained unchanged. Chaudhri and Singh [37] also suggested that the kaolinite in the Himalayan foreland basin originated from crystalline rocks containing feldspar and mica as also from pre-existing soils and sedimentary rocks. Analytical results also show that the chlorite groups are present in all the samples (Table 1), except A26 and A30 samples (Pleistocene paleosol samples) which contain vermiculites instead of chlorites. Illite concentrations show consistency with upper samples which contain chlorites. It is known that the vermiculites formed through the alteration of mica are comparatively rare in marine sediments because the K of seawater readily contracts them [32,66]. Consistency of illite concentration indicates that the initial sediments possibly contained micaceous minerals (chlorite, muscovite, and biotite) which were altered or degraded to vermiculites during subaerial weathering. Vermiculites are mainly formed by weathering of warm and humid climatic conditions [37] which are consistent with Al_2O_3 and Fe_2O_3 contents (Tables S5 and S6).
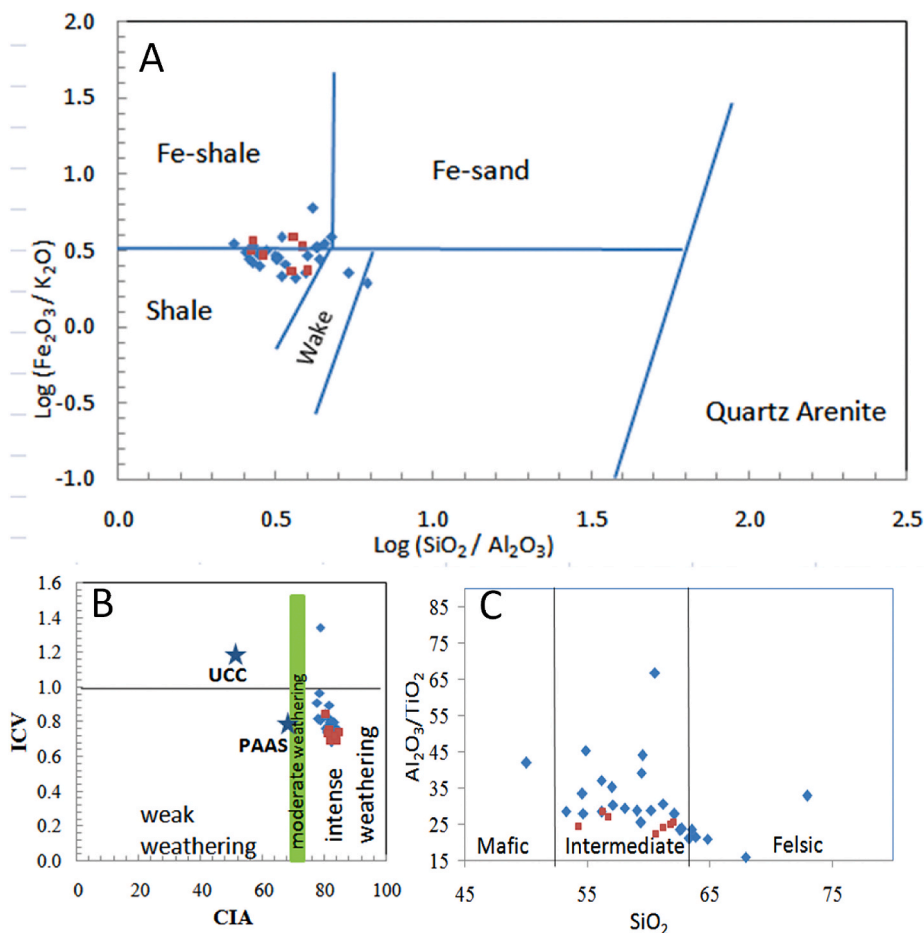
Fig. 7. (A) The plot of log (SiO2/Al2O3) versus log (Fe2O3/K2O) diagram by Ref. [93] classifies the samples mainly as Fe-rich shale, shale with some wake; (B) ICV (Index of Compositional Variability) versus CIA (Chemical Index of Alteration) plot for the sediments of the eastern coast of Bangladesh after [94]; where UCC (Upper Continental Crust) and PAAS (Post-Archean Australian Shale) values after [95] and (C) The plot of Al2O3/TiO2 versus SiO2 diagram classifies the samples mainly as Felsic to intermediate rock sources.

Lithological information indicates that the sediments (A26, A30) are characterized by greenish gray, light yellowish brown and gray, very sticky and very compact silty clay of -paleosol horizon (Tables S1 and S4) of the Pleistocene age. Hence, the presence of vermiculite suggests the subaerial weathering condition of deposition. The age of the paleosol is more than 10,000 yrs (Table S2). Ahsan et al. [96] also noted that the age of the underlying paleosol from the Bengal delta is more than 10,000 yrs. Chaudhri and Singh [37] suggested that the chlorite in the Himalayan foreland basin originated from the weathering of intermediate and basic crystalline rocks and low-grade metamorphic rocks in the source areas. Acharya and Paudyal [97] stated that chlorite is found in all pelagic rocks as a metamorphic index mineral of the Lesser Himalayas. Hossain et al. [6] stated that lithologically the strata exposed in the hills of CTFB are broadly similar to those exposed along the southern edge of the Sub-Himalayan orogenic belt. Gani and Alam and Najman et al. [34,98] stated that the Tertiary hills of CTFB consist of sediments that were deposited in the Bengal Basin from the Himalayan source, and subsequently uplifted and incorporated into the Neogene accretionary prism due to the oblique subduction of the oceanic crust of the Indian plate beneath the Myanmar sub-plate to the east during Pliocene. Therefore, like the Tertiary sediments, the present research also reveals that the recent unconsolidated coastal sediments of the area were also derived from the Himalayan source and the depositional environment was dominantly tidally influenced. The binary plot of Al_2O_3/TiO_2 versus SiO_2 (Fig. 7C) also indicates that the sedimentary processes in the area were sourced from the intermediate to felsic source-rock of the Himalayan [53]. The plot of ICV versus CIA indicates that the sediments seemingly experienced intense weathering in warm and humid climatic conditions (Fig. 7B). The area was tectonically active owing to the third Himalayan orogenic movement during the Miocene period [99]. The plots of Log (K_2O/Na_2O) versus SiO_2, TiO_2 versus Fe_2O_3+MgO, Al_2O_3/SiO_2 versus Fe_2O_3+MgO, and K_2O/Na_2O versus Fe_2O_3+MgO suggested that the sediments were mainly derived from the combined influence of active continental margin, continental island arc, and oceanic island arc zones (Fig. 8, [100,101]). It reflects the Himalayan linked complex Bengal Basin [4,34–36,50–52] depositional environment and tectonics.

5.2. Sea level change and sedimentation patterns

The measured ages reflect that the rate of deposition of sediments in the area varies from place to place and varies also with depth similar to other deltaic parts of the basin (Table 3). The reconstructed RSLC resembles [15,16] proposed curve i.e., after the LGM the sea level started to rise continuously and then reached its present position. Though, the upper half of the curve corresponds well to the curve reconstructed by Ref. [18].

6. Conclusions

The research reveals that the Tertiary hilly bed-rocks with undulated shaped morphology are commonly encountered at the immediate base of the Late Quaternary unconsolidated sediments (thickness ranges from 10 m to 50 m) or underneath the coastal plain having undulating topography. A sub-crop paleosol unit (Age: ≥10,000 yrs) is encountered over the bed-rock containing typical vermiculite mineral which indicates its sub-aerial weathering condition. This paleosol horizon is overlain by recent sediments. The analyzed lithologic, and sedimentologic characters, an abundance of typical Foraminiferal species and the presence of the clay-grouped minerals in the sequence suggest that the sediments were deposited in tidal conditions as well as fluvial influences during the Holocene time. The geochemical and mineralogical results indicate that presumably the analyzed sediments of the area were likely derived from the Himalayan intermediate to felsic-dominated metamorphic rock sources. These were experiencing intensive weathering (CIA: 77.8 to 84.6) related to the active uplift of the Himalayas. These have a recycled -orogen provenance linked to the tectonic setting of the active continental margin, continental island arc, and oceanic island. The sediments are classified as Fe-rich shale, shale, and wake, respectively. The analysis also reflects that the sedimentation rates of the area vary from place to place and layer to layer similar to other deltaic coastal parts of the Bengal basin due to complex delta formation. After the LGM, sediments of the area started to deposit on the top floor of the paleosol along with sea level rise under tidal, fluvial-tidal and fluvial influences. The reconstructed RSLC of the coast resembles [15,16] proposed curve, i.e., after the LGM the sea level rose incessantly to reach its current position. The output of the research will be helpful to understand the geological evolution of the recent coastal plain of the SE coast of the Bengal basin. Consequently, it will be supportive for researchers or planners for, land use planning, coastal management, and sustainable development of the area and so on. It would also be helpful to understand the possible sources of sediment input to the area from the complex interplay of the Indian-, Eurasian- and Myanmar-plates.

Author contribution statement

Md. Bazlar Rashid, PhD: Conceived and designed the experiments; Performed the experiments; Analyzed and interpreted the data; Contributed reagents, materials, analysis tools or data; Wrote the paper.

Md. Ahosan Habib, PhD: Performed the experiments; Analyzed and interpreted the data; Contributed reagents, materials, analysis tools or data.

Arif Mahmud, MSc; Md. Kamrul Ahsan, MSc; Md. Hossain Khasru, MSc; Md. Ashraf Hossain, MSc; Aktarul Ahsan, MSc; Kazi Munsura Akther; Shawon Talukder: Contributed reagents, materials, analysis tools or data.
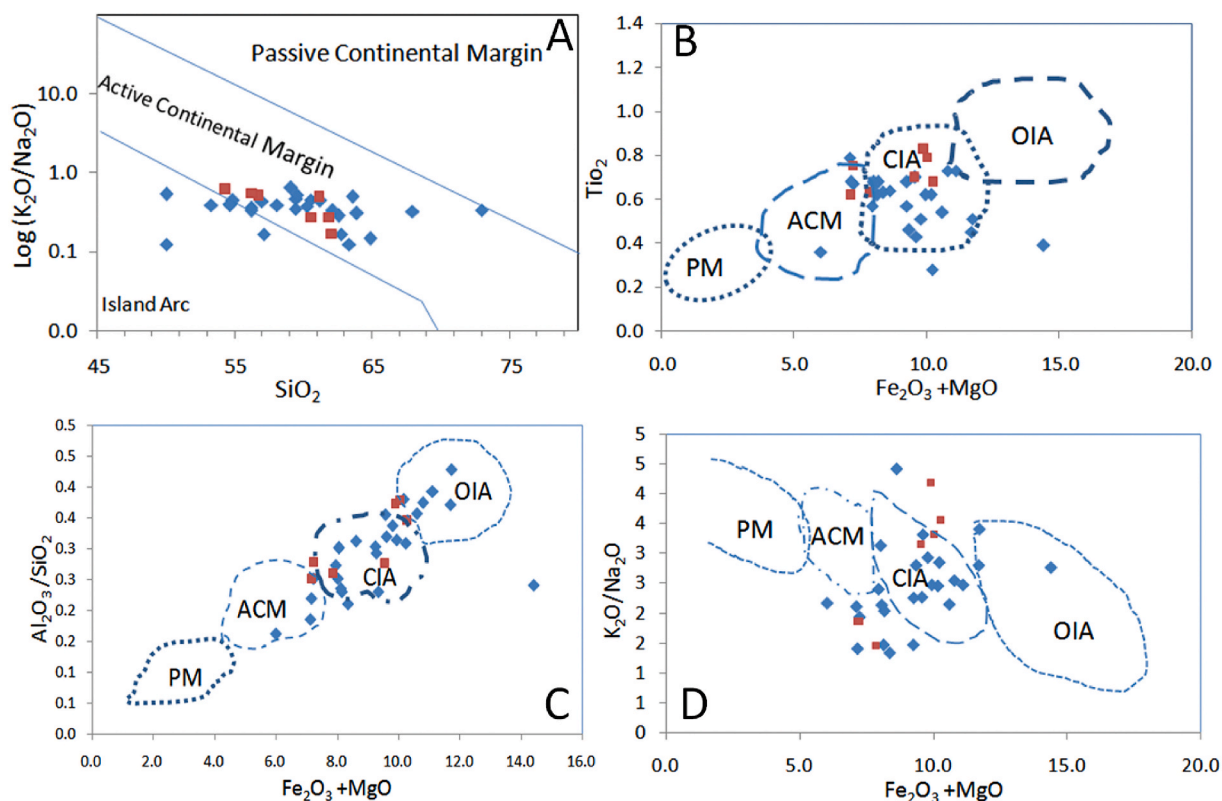
Fig. 8. Tectonic-setting discrimination diagrams for the sediments of the eastern coast of Bangladesh, boundaries of fields are from Ref. [100] (A) [101]; for (B), (C) and (D), where PM = passive margin, ACM = active continental margin, IA = island arc, CIA = continental island arc, OIA = oceanic island arc.

Data availability statement

Data will be made available on request.

Declaration of interest's statement

The authors declare that they have no known competing financial interests or personal relationships that could have appeared to influence the work reported in this paper.

Acknowledgments

Appendix A. Supplementary data

Supplementary data related to this article can be found at https://doi.org/10.1016/j.heliyon.2023.e12998.

References

[1] D.K. Guha, Tectonic framework and oil and gas prospects of Bangladesh, in: 4th Annual Conference Proceedings, Bangladesh Geological Society, 1978, pp. 65–76.

[2] M.R. Khan, Tectonics and Bangladesh, J. Asiatic Soc. Bangladesh Sci. 28 (2) (2002) 39–62. Golden Jubilee Issue, Dhaka, Bangladesh.

[3] K.U. Reimann, Geology of Bangladesh, Gebruder Borntrager, Berlin, 1993, p. 160.

[4] M. Alam, M.M. Alam, J.R. Curray, M.L.R. Chowdhury, M.R. Gani, An overview of the sedimentary geology of the Bengal Basin in relation to the regional tectonic framework and basin-fill history, Sediment. Geol. 155 (2003) 179–208.

[5] M.J.J. Rahman, W. Xiao, T. McCann, A. Songjian, Provenance of the Neogene Surma group from the Chittagong Tripura Fold Belt, southeast Bengal Basin, Bangladesh: constraints from whole-rock geochemistry and detrital zircon U-Pb ages, J. Asian Earth Sci. 148 (2017) 277–293.

[6] M.S. Hossain, M.S.H. Khan, K.R. Chowdhury, R. Abdullah, Synthesis of the tectonic and structural elements of the Bengal Basin and its surroundings, in: S. Mukherjee (Ed.), Tectonics and Structural Geology: Indian Context, Springer, Cham, 2019, pp. 135–218, https://doi.org/10.1007/978-3-319-99341-6_6.

[7] S.R. Khan, Geomorphic and geologic characteristics of the coastal plains of Bangladesh, in: Proceedings of the international Seminar on-Quaternary Developments and Coastal Hydrodynamics of the Ganges Delta in Bangladesh 57, 2001.

[8] M.A. Islam, A.B.K. Majlis, M.B. Rashid, Changing face of Bangladesh coast, J. NOAMI 28 (1) (2011) 1–17.

[9] M.B. Rashid, A. Mahmud, Longshore currents and its effect on Kuakata beach, Bangladesh, Bangladesh J. Geol. 29–30 (2011) 30–40.

[10] M.B. Rashid, A. Mahmud, M.K. Ahsan, M.H. Khasru, M.A. Islam, Drainage congestion and its impact on environment in the South-western coastal part of Bangladesh, Bangladesh J. Geol. 31–32 (2013) 43–55.

[11] S. Rahman, M.A. Rahman, Climate extremes and challenges to infrastructure development in coastal cities in Bangladesh, Weather Clim. Extrem. 7 (2015) 96–108, https://doi.org/10.1016/j.wace.2014.07.004.

[12] B.K. Paul, H. Rashid, Coastal landform changes: coastal erosion, land accretion and subsidence, Clim. Hazards Coast. Bangladesh (2017) 121–152. Book chapter.

[13] M.A.B. Siddique, R. Khan, A.R.M.T. Islam, M.K. Alam, M.S. Islam, M.S. Hossain, M.A. Habib, M.A. Akbor, U.H. Bithi, M.B. Rashid, M. Hossain, I.M.M. Rahman, I.B. Elius, M.S. Islam, Quality Assessment of Freshwaters from a Coastal City of Southern Bangladesh: Irrigation Feasibility and Preliminary Health Risks Appraisal, Environmental Nanotechnology, Monitoring and Management, Elsevier, 2021, https://doi.org/10.1016/j.enmm.2021.100524, 16, https://www.sciencedirect.com/science/article/pii/S2215153221000994.

[14] M. Umitsu, Natural levees and landform evolutions in the Bengal lowland, Geogr. Rev. Jpn. B 58 (1985) 149–164.

[15] M. Umitsu, Late Quaternary sedimentary environment and landform evolution in the Bengal lowland, Geogr. Rev. Jpn. 60 (1987) 164–178.

[16] M. Umitsu, Late Quaternary sedimentary environments and landforms in the Ganges Delta, Sedimentary Geology vol. 83 (1993) 177–186.

[17] I.B. Singh, Geological evolution of Ganga plain-An overview, J. Paleontol. Soc. India 41 (1996) 99–137.

[18] S.L. Goodbred Jr., S.A. Kuehl, The significance of large sediment supply, active tectonism, and eustasy on margin sequence development: late Quaternary stratigraphy and evolution of the Ganges-Brahmaputra delta, Sediment. Geol. 133 (3–4) (2000) 227–248, https://doi.org/10.1016/S0037-0738(00)00041-5.

[19] R. Sinha, S.K. Tandon, M.R. Gibling, P.S. Bhattacharjee, A.S. Dasgupta, Late Quaternary geology and alluvial stratigraphy of the Ganga basin, J. Himal. Geol. 26 (2005) 223–240.

[20] M.B. Rashid, A. Mahmud, M.K. Ahsan, M.H. Khasru, K. Ahsan, M.A. Habib, M.A. Hossain, M.F. Alam, Role of major rivers for the development of Ganges-Brahmaputra delta, Int. J. Econ. Environ. Geol. 5 (1) (2014) 25–32.

[21] M.A. Allison, S.R. Khan, S.L. Goodbred Jr., S.A. Kuehl, Stratigraphic evolution of the late Holocene Ganges-Brahmaputra lower delta plain, Sediment. Geol. 155 (3–4) (2003) 317–342.

[22] H.M. Masidul, H. Koichi, Influences of sea level on depositional environment during the last 1000 years in the southwestern Bengal delta, Bangladesh, Holocene (2021), https://doi.org/10.1177/0959683621994671.

[23] H.Z. Hossain, Q.H. Hossain, A. Kamei, D. Araoka, Compositional variations, chemical weathering, and provenance of sands from the Cox's Bazar and Kuakata beach areas, Bangladesh, Arabian J. Geosci. 11 (23) (2018) 1–17.

[24] M.S.H. Khan, B. Parkash, S. Kumar, Soil-landform development of a part of the fold belt along the eastern coast of Bangladesh, Geomorphology 71 (3–4) (2005) 310–327.

[25] A.K.M.S. Hasan, J. Hasan, Geomorphology of the east coastal zone of Bangladesh, J. NOAMI 19 (2) (2002) 1–25.

[26] S.R. Khan, M.A. Ali, A.B.K. Majlis, Morphological evolution of Holocene coastal plain of coxs Bazar-Teknaf area, southeast Bangladesh, Bangladesh J. Geol. 25 (2006).

[27] K. Ahsan, M.B. Rashid, M.A. Habib, M.F. Alam, The changing geometry of the Cox's Bazar-Badarmokam coast, Bangladesh, Bangladesh J. Geol. 26–28 (2009) 25–36.

[28] K. Ahsan, M.B. Rashid, Coastal process in the Cox's Bazar-Teknaf area of the eastern coast of Bangladesh, Book of Abstracts, ISBN: 978-85-64964-09-9, Ninth International Conference on Coastal and Port Engineering in Developing Countries (PIANC-COPEDEC IX), 16 Oct-21Oct 2016, Rio De Jeneiro, Brazil, www.pianc-copedec2016.com.br, 2016, 118.

[29] M.H. Monsur, A.S.M.M. Kamal, Holocene Sea level changes along the Maheskhali and Cox's Bazar- Teknaf coast of the Bay of Bengal, J. NOAMI 11 (1) (1994) 15–21.

[30] C.E. Weaver, Geologic interpretation of argillaceous sediments, Pt. I, origin and significance of clay minerals in sedimentary rocks, Bull. Am. Assoc. Petrol. Geol. 42 (2) (1958) 254–271.

[31] G. Millot, Geology of Clays, Springer-Verlag, NewYork, 1970.

[32] W.A. Deer, R.A. Howie, J. Zussman, An Introduction to Rock-Forming Minerals, Longman Group Ltd., London, 1975, p. 528.

[33] L.A. Stern, C.P. Chamberlain, R.C. Reynolds, G.D. Johnson, Oxygen isotope evidence from Pedogenic clay minerals in the Himalayan Molasse, Geochem. Cosmochim. Acta 61 (4) (1997) 731–744, https://doi.org/10.1016/S0016-7037(96)00367-5.

[34] M. Gani, M.M. Alam, Trench-slope controlled deep-sea clastics in the exposed lower Surma group in the southeastern fold belt of the Bengal Basin, Bangladesh, Sediment. Geol. 127 (1999) 221–236.

[35] M.R. Gani, M.M. Alam, Sedimentation and basin-fill history of the Neogene clastic succession exposed in the southeastern fold belt of the Bengal Basin, Bangladesh: a high-resolution sequence stratigraphic approach, Sediment. Geol. 155 (3–4) (2003) 227–270.

[36] C. Davies, J. Best, R. Collier, Sedimentology of the Bengal shelf, Bangladesh: comparison of late Miocene sediments, Sitakund anticline, with the modern, tidally dominated shelf, Sediment. Geol. 155 (3–4) (2003) 271–300.

[37] A.R. Chaudhri, M. Singh, Clay minerals as climate change indicators-A case study, Am. J. Clim. Change 1 (2012) 231–239, https://doi.org/10.4236/ajcc.2012.14020. http://www.SciRP.org/journal/ajcc) 231.

[38] E. Garzanti, The maturity myth in Sedimentology and provenance analysis, J. Sediment. Res. 87 (2017) 353–365, https://doi.org/10.2110/jsr.2017.17.

[39] E. Garzanti, Petrographic classification of sand and sandstone, Earth Sci. Rev. (2019), https://doi.org/10.1016/J.EARSCIREV.2018.12.014.

[40] X. Cui, S. Li, H. Xu, Z. Zhang, X. Zhao, Z. Gao, N. Wei, X. Zhang, Late quaternary Paleoenvironmental reconstruction, using benthic foraminifera and Ostracoda, of marine sedimentary beds on the southern coast of Laizhou Bay, Bohai Sea, China, J. Foraminifer. Res. 48 (2) (2018) 87–99.

[41] A.D. Switzer, R.P. Felix, J.L.A. Soria, T.A. Shaw, A comparative study of the 2013 typhoon Haiyan overwash sediments from a coastal cave and beach system at Salcedo, Eastern Samar, central Philippines, Mar. Geol. 419 (2020), 106083.

[42] A.O. Amao, M.A. Qurban, M.A. Kaminski, T.V. Joydas, P.K. Manikandan, F. Frontalini, A baseline investigation of benthic foraminifera in relation to marine sediments parameters in western parts of the Arabian Gulf, Mar. Pollut. Bull. 146 (2019) 751–766.

[43] J.R. Curray, The Bengal depositional system: from rift to orogeny, Mar. Geol. 352 (2014) 59–69.

[44] A. Mukherjee, A.E. Fryar, W.A. Thomas, Geologic, geomorphic and hydrologic framework and evolution of the Bengal basin, India and Bangladesh, J. Asian Earth Sci. 34 (2009) 227–244.

[45] A.K. Jain, D.M. Banerjee, V.S. Kale, Geology and tectonics of Bangladesh, in: Tectonics of the Indian Subcontinent, Society of Earth Scientists Series, Springer, Cham, 2020, https://doi.org/10.1007/978-3-030-42845-7-10.

[46] J.P. Morgan, W.G. McIntire, Quaternary Geology of the Bengal Basin, East Pakistan and India, Bull. Geol. Soc. Am. 70 (1959) 319–341.

[47] R.A. Khandoker, Development of major tectonic elements of the Bengal Basin: a tectonic appraisal, Bangladesh J. Sci. Res. 7 (1989) 221–232.

[48] D.R. Nandy, Geodynamics of Northeast India and the Adjoining Region, ABC Publications, Calcutta, 2001, pp. 1–209.

[49] A.B. Roy, A. Chatterjee, Tectonic framework and evolutionary history of the Bengal Basin in the Indian subcontinent, Curr. Sci. 109 (2015) 271–279.

[50] A.A. Khan, Tectonics of the Bengal Basin, J. Himal. Geol. 2 (1) (1991) 91–101.

[51] A. Uddin, N. Lundberg, Miocene sedimentation and subsidence during continent-continent collision, Bengal basin, Bangladesh, Sediment. Geol. 164 (2004) 131–146.

[52] P.G. DeCelles, P. Kapp, G.E. Gehrels, L. Ding, Paleocene-Eocene foreland basin evolution in the Himalaya of southern Tibet and Nepal: implications for the age of initial India-Asia collision, Tectonics 33 (2014) 824–849.

[53] M. Begum, R. Khan, D.K. Roy, M.A. Habib, M.B. Rashid, K. Naher, M.A. Islam, U. Tamim, S.C. Das, S.M. Al Mamun, M.S. Hossain, Geochemical characterization of miocene core sediments from Shahbazpur gas-wells (Bangladesh) in terms of elemental abundances by instrumental neutron activation analysis, J. Radioanal. Nucl. Chem. (2021), https://doi.org/10.1007/s10967-021-07770-4.

[54] S.A. Kuehl, T.M. Hairu, W.S. Moore, Shelf sedimentation of the Ganges-Brahmaputra river system-evidence for sediment bypassing to the Bengal Fan, Geology 17 (1989) 1132–1135.

[55] S.L. Goodbred Jr., S.A. Kuehl, Floodplain processes in the Bengal Basin and the storage of Ganges-Brahmaputra river sediment: an accretion study using 137Cs and 210Pb geochronology, Sediment. Geol. 121 (1998) 239–258.

[56] J. Troels-Smith, Characterization of unconsolidated sediment, Danmarks Geologiske Undersogelse, IV 3 (1955) 38–73.

[57] C.S. Agarwal, P.K. Garg, Textbook on Remote Sensing in Natural Resources Monitoring and Management, Wheeler Publishing, New Delhi, India, 2000.

[58] M.B. Rashid, Channel bar development and bankline migration of the Lower Padma River of Bangladesh, Arabian J. Geosci. 13 (2020) 612, https://doi.org/10.1007/s12517-020-05628-9.

[59] M.B. Rashid, M.A. Habib, R. Khan, A.R.M.T. Islam, Land transform and its consequences due to the route change of the Brahmaputra River in Bangladesh, Int. J. River Basin Manag. (2021), https://doi.org/10.1080/15715124.2021.1938095.

[60] M.B. Rashid, M.A. Habib, Channel bar Development, Braiding and Bankline Migration of the Brahmaputra-Jamuna River, Bangladesh through RS and GIS techniques, Int. J. River Basin Manag. (2022), https://doi.org/10.1080/15715124.2022.2118281.

[61] A. Goto, Y. Tatsumi, Quantitative analysis of rock samples by an X-ray fluorescence spectrometer (I), Rigaku J. 11 (1994) 40–59.

[62] R.I. Barnhisel, P.M. Bertsch, Chlorites and Hydroxy-interlayered vermiculite and Smectite, in: J.B. Dixon, S.B. Weed (Eds.), Minerals in Soil Environments, Soil Science Society of America Book Series, Madison, WI, 1989, pp. 729–788.

[63] G. Brown, G.W. Brindly, X-ray diffraction procedure for clay mineral identification, in: G.W. Brindley, G. Brown edited (Eds.), Crystal Structures of Clay Minerals and Their X-Ray Identification, Mineralogical Society, 1980, pp. 305–356.

[64] J.J. Griffin, H. Windom, E.D. Goldberg, The distribution of clay minerals in the World Ocean, Deep Sea Res. Oceanogr. Abstr. 15 (4) (1968) 433–459, https://doi.org/10.1016/0011-7471(68)90051-X.

[65] D. Carroll, Clay minerals: a Guide to their identification, Geol. Soc. Am. 126 (1970) 48–55.

[66] D.M. Moore, R.C. Reynolds Jr., X-Ray Diffraction and the Identification and Analysis of Clay Minerals, second ed., Oxford university Press, New York, 1997, p. 378.

[67] Douglas, A laboratory manual for X-ray powder diffraction, coastal and marine geology Program, U.S. Geological Survey Open-File Report 01-041, Chlorite Group, URL: http://pubs.usgs.gov/of/2001/of01-041/htmldocs/clays/verm.htm, 1989. Last modified on 11 Oct, 2001.

[68] Swindale, X-Ray powder diffraction patterns of oriented-aggregate mounts showing the effects of standard treatments on : kaolinite, Dickite, A laboratory manual for X-ray Powder diffraction, coastal and marine geology Program, U.S. Geological Survey Open-File Report 01-041, Chlorite Group, URL: http://pubs.usgs.gov/of/2001/of01-041/htmldocs/clays/verm.htm, 1975. Last modified on 11 Oct, 2001.

[69] P.E. Biscaye, Mineralogy and sedimentation of recent deep sea clays in the atlantic ocean and adjacent seas and oceans, Geol. Soc. Am. Bull. 76 (1965) 803–832.

[70] M. Delage, Hérouard, in: World Register of Introduced Marine Species (WRiMS), 1896.

[71] J.V. Cushman, Foraminifera, Their Classification and Economic Use, University Press, Cambridge-Massachusetts-Harvard, 1959, pp. 1–589.

[72] S.T. Ahmed, Tertiary Foraminifera from the Inani Anticline, Cox's Bazar VI, The Rajshahi University Studies, 1975, pp. 248–266.

[73] A.R. Loeblich, H. Tappan, Treatise on Invertebrate Paleontology, Part C: Protista 2, Sarcodina, Chiefly "Thecamoebians" and Foraminiferida, Geological Society of America and University of Kanzas Press, Lawrence, 1964.

[74] V. Pokorny, Principle of zoological Micropaleontology, Int. Monogr. Earth Sci. 1 (1963) 45–109.

[75] A.F.M. Haque, Mohsenul, The Smaller Foraminifera of the Ranikot and Laki of the Nammal Gorge, Salt Range, Palaontologia Pakistanica, Pakistan, Memories of Geological Survey of Pakistan. I, 1956.

[76] M.D. Brasier, Microfossils, George Allen and Unwin Ltd., 1980, pp. 90–121.

[77] R.E. Taylor, Radiocarbon Dating, Academic Press, London, 1987, ISBN 978-0-12-433663-6.

[78] J. Southon, M. Kashgarian, M. Fontugne, B. Metivier, W. W-S Yim, Marine reservoir corrections for the Indian ocean and southeast asia, Radiocarbon 44 (1) (2002) 167–180, https://doi.org/10.1017/S0033822200064778.

[79] Vishnu-Mittre, H.P. Guputa, Pollen analytical study of quaternary deposits in the Bengal Basin, Paleobotanist 19 (1970) 297–306.

[80] A.K. Hait, H.K. Das, S. Ghosh, A.K. Ray, A.K. Saha, S. Chanda, New dates of Pleisto-Holocene subcrop samples from south Bengal, India, Indian J. Earth Sci. 23 (1996) 79–82.

[81] D.J. Stanley, A.K. Hait, Holocene depositional patterns, neotectonics and Sunderbans mangroves in the western Ganges-Brahmaputra delta, J. Coast Res. 14 (2000) 794–825.

[82] H.P. Gupta, Palaeoenvironments during Holocene time in Bengal Basin, India as reflected by palynostratigraphy, Paleobotanist 27 (1981) 138–160.

[83] H. Brammer, Coatings in seasonally flooded soils, Geoderma 6 (1971) 5–16.

[84] H.W. Nesbitt, G.M. Young, Early Proterozoic climates and plate motions inferred from major element chemistry of lutites, Nature 96 (1982) 715–717.

[85] Weaver, A Discussion on the Origin of Clay Minerals in Sedimentary Rocks, Shell Oil Company, Houston, Texas, 1956.

[86] M.A. Habib, R. Khan, K. Phoungthong, Evaluation of environmental radioactivity in soils around a coal burning power plant and a coal mining area in Barapukuria, Bangladesh: Radiological risks assessment, Chem. Geol. 600 (2022) 120865, https://doi.org/10.1016/j.chemgeo.2022.120865.

[87] R. Cox, D.R. Lowe, R.L. Cullers, The influence of sediment recycling and basement composition on evolution of mudrock chemistry in the southwestern United States, Geochem. Cosmochim. Acta 59 (14) (1995) 2919–2940, https://doi.org/10.1016/0016-7037(95)00185-9.

[88] M. Gharrabi, B. Velde, J.P. Sagon, The transformation of illite to muscovite in pelitic rocks: constraints from X-ray diffraction, Clay Clay Miner. 46 (1) (1998) 79–88.

[89] J.R.L. Allen, Mud drapes in sand-wave deposits: a physical model with application to the Folkestone Beds (early Cretaceous, southeast England), Philos. Trans. Roy. Soc. Lond. Math. Phys. Sci. 306 (1493) (1982) 291–345.

[90] R. Coueffe, B. Tessier, P. Gigot, B. Beaudoin, Tidal rhythmites as possible indicators of very rapid subsudence in a foreland basin: an example from the Miocene marine moalsse formation of the Digne foreland basin, Se France, J. Sediment. Res. 74 (6) (2004) 2–15.

[91] R. Mazumder, M. Arima, Tidal rhythmites and their implications, Earth Sci. Rev. 69 (1–2) (2005) 79–95, https://doi.org/10.1016/j.earscirev.2004.07.004.

[92] J.W. Murray, Ecology and Applications of Benthic Foraminifera, Cambridge university press, 2006.

[93] M.M. Herron, Geochemical classification of terrigenous sands and shales from core or log data, J. Sediment. Petrol. 58 (1988) 820–829, https://doi.org/10.1306/212F8E77-2B24-11D7-8648000102C1865D.

[94] X. Long, C. Yuan, M. Sun, W. Xiao, Y. Wang, K. Cai, Y. Jiang, Geochemistry and Nd isotopic composition of the Early Paleozoic flysch sequence in the Chinese Altai, Central Asia: evidence for a northward-derived mafic source and insight into model ages in an accretionary orogen, Gondwana Res. 22 (2012) 554–566.

[95] S.R. Taylor, S.M. McLennan, The Continental Crust: its Composition and Evolution, Blackwell, Oxford, 1985, pp. 1–312.

[96] K.M. Ahsan, M.H. Khasru, M.B. Rashid, Geology of the Western Part of Khulna District and Satkhira District, Bangladesh (In Compliance with the Project of Geological Exploration for the Identification of Mineral Resources and the Areas Vulnerable to Natural Hazards in the Coastal Parts of Bangladesh), Unpublished, Records of the Geological Survey of Bangladesh, GSB/DATA/UR-753, 2014.

[97] R.K. Acharya, K.R. Paudyal, Petrography of Low-Grade Metamorphic Rocks of the Lesser Himalaya from Malekhu Area, Central Nepal, 2015, https://doi.org/10.3126/jsce.v3i0.22385.

[98] Y. Najman, R. Allen, E.A.F. Willett, A. Carter, D. Barfod, E. Garzanti, J. Wijbrans, M.J. Bickle, G. Vezzoli, S. Ando, G. Oliver, The record of Himalayan erosion preserved in the sedimentary rocks of the Hatia trough of the Bengal Basin and the Chittagong hill Tracts, Bangladesh, Basin Res. 24 (5) (2012) 499–519, https://doi.org/10.1111/j.1365-2117.2011.00540.x.

[99] M.S. Krishnan, Geology of India and Burma, Published by White Lotus Press, Madras, 1960.

[100] B.P. Roser, R.J. Korsch, Determination of tectonic setting of sandstone mudstone suites using SiO_2 content and K_2O/Na_2O ration, J. Geol. 94 (1986) 635–650.

[101] M.R. Bhatia, Plate tectonics and geochemical composition of sandstones, J. Geol. 92 (1983) 181–193, https://doi.org/10.1086/628815.